Int. J. Heat Mass Transfer. Vol. 35, No. 11, pp. 2953–2962, 1992
Printed in Great Britain

0017–9310/92 $5.00+0.00

Analysis of transient behaviour of multipass shell and tube heat exchangers with the dispersion model

W. ROETZEL and Y. XUAN

Institute of Thermodynamics, University of the Federal Armed Forces Hamburg, Holstenhofweg 85, D-2000 Hamburg 70, F.R.G.

(*Received* 26 *September* 1991)

Abstract—To take the effect of shellside flow maldistributions into account, the dispersion model is used for predicting the transient behaviour subject to arbitrary inlet temperature changes in multipass shell and tube heat exchangers. The number and size of tubeside passes are arbitrary and two possible flow arrangements are considered. Besides the thermal capacities of both fluids and the core wall, the thermal capacity of the shell wall is included in the model. The final solution is obtained by means of the numerical inverse Laplace transform. The influence of the shellside flow maldistribution and the thermal capacity of the shell wall are discussed.

INTRODUCTION

MORE AND more research papers have contributed to the analysis of the transient behaviour of shell and tube heat exchangers, since the knowledge of dynamic characteristics of such equipment is elementary information for the design of control systems to achieve the optimum design and operation. Correa and Marchetti [1] applied the concept of cell structure to describing the dynamic behaviour of multipass shell and tube heat exchangers subject to a step inlet temperature change, in which the influence of the thermal capacity of the core wall was considered by introducing an equivalent tubeside specific heat capacity. By means of a numerical inverse Laplace transform, the authors of this paper developed a method [2] for predicting the transient responses to arbitrary inlet temperature changes of multipass shell and tube heat exchangers with an arbitrary number of tubeside passes and finite thermal capacities of both the fluids and the core wall. However, all these papers are based upon the ideal plug-flow model. This conventional model may fail if strong shellside flow maldistributions occur which degrade the performance of equipment.

In fact, the shellside flow is never uniform because of the complicated geometrical structures such as baffles and windows. Mueller [3] classified the various kinds of possible flow maldistributions in heat exchangers. The effect of these maldistributions on the thermal performance of the exchanger depends on the intensity of each maldistribution. The dispersion model is a very effective instrument to estimate the effect of flow maldistributions on the performance under the stationary condition [4, 5].

The dispersion model is an improved plug-flow model, i.e. it is based on the main plug-flow with axial diffusion or dispersion which may be both molecular and macroscopic (laminar or turbulent). The synonym of axial dispersion is back-mixing. In this model, the apparent axial heat conduction term is introduced into the energy balance and the effect of flow maldistribution is taken into account by this dispersion term in the energy equation. It is convenient and accessible to use this one-dimensional model with only the axial space variable to handle such problems concerning complicated flow patterns. Taylor [6] may be the first to develop the dispersion model for mass transfer in turbulent flow through a pipe.

In this paper, the application of the dispersion model is extended to the transient analysis of multipass shell and tube heat exchangers. In the light of this model, the expressions for the transient responses to arbitrary inlet temperature changes in exchangers with N tubeside passes (designated as $1-N$) are derived. The thermal capacities of both fluids, the core wall and the shell as well as two possible flow arrangements are included. The fact that the thermal properties and the number of transfer units (NTU) vary piecewise from pass to pass is allowed for. The final solutions are obtained by means of the numerical inverse Laplace transform. According to the derived expressions, the effect of the shellside flow maldistribution on the transient behaviour of such apparatus is analysed.

DERIVATION OF THE GOVERNING EQUATIONS

The previous analysis [7] has shown that the effect of longitudinal heat conduction in the wall is generally negligible, so that such longitudinal heat conduction will be neglected in the following derivations. The other necessary assumptions are listed as follows:

(1) the thermal flow rates $\dot{W}_1$ and $\dot{W}_2$ of both fluids are constant;

NOMENCLATURE

A	heat transfer surface area [m^2]
C	heat capacity [J K^{-1}]
D	dispersion coefficient or apparent heat conductivity [W m^{-1} K^{-1}]
$f_1(z), f_2(z)$	inlet temperature changes
$F_1(s), F_2(s)$	transformed forms of $f_1(z)$ and $f_2(z)$ in the image domain
$g_j(x)$	steady parts defined in equation (30)
h	heat transfer coefficient [W m^{-2} K^{-1}]
l	distance from the entrance of shellside fluid [m]
L	length of the heat exchanger [m]
M	number of the summed series terms in equation (27)
N	number of tubeside passes
NTU	number of transfer units, dimensionless
Pe	Péclet number defined in equation (6)
s	parameter of the Laplace transform
t	dimensionless temperature, $t = (\theta-\theta_0)/(\theta_r-\theta_0)$
T	transformed form of t in the Laplace transform domain
$\dot{W}$	thermal flow rate [W K^{-1}]
x	dimensionless coordinate, $x = l/L$
z	dimensionless time.

Greek symbols

θ	temperature [K]
θ_0	initial temperature in heat exchangers [K]
θ_r	reference temperature [K]
λ	eigenvalue
τ	time [s]
τ_r	residence time of fluid in the heat exchanger [s]
$\phi_j(x, z)$	transient parts defined in equation (31).

Subscripts

1	shellside fluid
2	tubeside fluid
e	exit
n	new inlet temperature change
q	cross-section
s	shell wall
w	core wall.

Superscripts

$'$	inlet
$''$	exit.

(2) the wall heat transfer resistance is negligible, compared with the convective heat transfer resistances on both sides;

(3) the effect of shellside flow maldistribution can be described by introducing a dispersion term in the shellside energy equation; and

(4) no heat is transferred from the shell of the exchanger to the environment.

The shell and tube heat exchangers with N tubeside passes and two different tubeside flow arrangements are illustrated in Fig. 1. The origin of the coordinate system is always set at the location where the shellside fluid enters the apparatus. According to the above-mentioned presumptions, one is able to derive the following differential equations:

$$\frac{A_q D}{L}\frac{\partial^2 t_1}{\partial x^2} - \dot{W}_1\frac{\partial t_1}{\partial x} - C_1\frac{\partial t_1}{\partial \tau} - \sum_{i=1}^{N}(hA)_{1i}(t_1 - t_{wi}) - (hA)_s(t_1 - t_s) = 0 \quad (1)$$

$$\pm(-1)^i \dot{W}_{2i}\frac{\partial t_{2i}}{\partial x} + C_{2i}\frac{\partial t_{2i}}{\partial \tau} + (hA)_{2i}(t_{2i} - t_{wi}) = 0 \quad (i = 1, 2, \ldots, N) \quad (2)$$

$$C_{wi}\frac{\partial t_{wi}}{\partial \tau} - (hA)_{1i}(t_1 - t_{wi}) - (hA)_{2i}(t_{2i} - t_{wi}) = 0 \quad (i = 1, 2, \ldots, N) \quad (3)$$

$$C_s\frac{\partial t_s}{\partial \tau} = (hA)_s(t_1 - t_s) \quad (4)$$

where the positive sign $(+)$ and negative sign $(-)$ of $(\pm)$ in equation (2) are valid for tubeside flow arrangements I and II which are shown in Fig. 1, respectively.

According to the first assumption, the thermal flow rate $\dot{W}_2$ does not change from pass to pass. But the thermal capacity C_{2i} of the tubeside fluid may be different from pass to pass. The residence times τ_{r1} and τ_{r2} of both fluids and some dimensionless parameters are introduced

$$\tau_{r1} = \frac{C_1}{\dot{W}_1}, \quad \tau_{r2} = \frac{C_2}{\dot{W}_2}, \quad \tau_{r2i} = \frac{C_{2i}}{\dot{W}_{2i}}$$

$$R_1 = \frac{\dot{W}_1}{\dot{W}_2} = \frac{1}{R_2}, \quad U_1 = \frac{(hA)_1}{\dot{W}_1}, \quad U_2 = \frac{(hA)_2}{\dot{W}_2},$$

$$U_{1i} = \frac{(hA)_{1i}}{\dot{W}_1}, \quad U_{2i} = \frac{(hA)_{2i}}{\dot{W}_2}, \quad U_s = \frac{(hA)_s}{\dot{W}_1},$$

$$NTU_1 = \left[\frac{1}{(hA)_1} + \frac{1}{(hA)_2}\right]^{-1}\frac{1}{\dot{W}_1} = \frac{U_1 U_2 R_2}{U_1 + U_2 R_2},$$

$$\varepsilon_{1i} = \frac{(hA)_{1i}}{(hA)_1} = \frac{U_{1i}}{U_1}, \quad \varepsilon_{2i} = \frac{(hA)_{2i}}{(hA)_2} = \frac{U_{2i}}{U_2},$$

$$\varepsilon_{ci} = \frac{C_{2i}}{C_2}, \quad \varepsilon_{wi} = \frac{C_{wi}}{C_w}$$

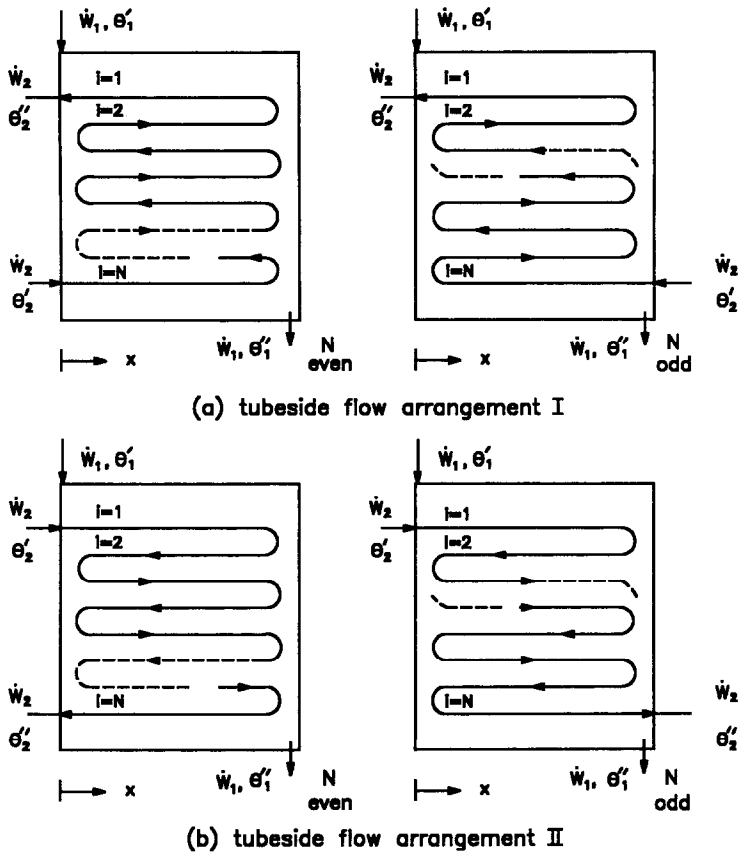

FIG. 1. Schematic representation of multipass shell and tube heat exchangers.

where

$$(hA)_1 = \sum_{i=1}^{N} (hA)_{1i}, \quad (hA)_2 = \sum_{i=1}^{N} (hA)_{2i},$$

$$C_2 = \sum_{i=1}^{N} C_{2i} \quad \text{and} \quad C_w = \sum_{i=1}^{N} C_{wi}.$$

Obviously, there are the following relationships:

$$\sum_{i=1}^{N} \varepsilon_{1i} = 1, \quad \sum_{i=1}^{N} \varepsilon_{2i} = 1, \quad \sum_{i=1}^{N} \varepsilon_{ci} = 1,$$

$$\sum_{i=1}^{N} \varepsilon_{wi} = 1 \quad \text{and} \quad \tau_{r2i} = \varepsilon_{ci}\tau_{r2}. \tag{5}$$

The other dimensionless parameters are defined as

$$R_\tau = \frac{\tau_{r2}}{\tau_{r1}}, \quad R_{c1} = \frac{C_1}{C_2} = \frac{R_1}{R_\tau} = \frac{1}{R_{c2}},$$

$$R_w = \frac{C_w}{C_1 + C_2}, \quad R_{wi} = \frac{C_{wi}}{C_1 + C_2},$$

$$R_s = \frac{C_s}{C_w}, \quad \alpha_{1i} = \frac{U_{1i}}{1 + R_{c2}},$$

$$\alpha_{2i} = \frac{U_{2i}}{R_\tau(1 + R_{c1})}, \quad \text{sign} = \pm(-1)^i.$$

Introducing the dimensionless time variable $z = \tau/\tau_{r1}$, one can rewrite equations (1)–(4) as follows:

$$\frac{1}{Pe}\frac{\partial^2 t_1}{\partial x^2} - \frac{\partial t_1}{\partial x} - \frac{\partial t_1}{\partial z} - \sum_{i=1}^{N} U_{1i}(t_1 - t_{wi}) - U_s(t_1 - t_s) = 0 \tag{6}$$

$$\text{sign}\frac{\partial t_{2i}}{\partial x} + \varepsilon_{ci} R_\tau \frac{\partial t_{2i}}{\partial z} + U_{2i}(t_{2i} - t_{wi}) = 0 \tag{7}$$

$$R_{wi}\frac{\partial t_{wi}}{\partial z} - \alpha_{1i}(t_1 - t_{wi}) - \alpha_{2i}(t_{2i} - t_{wi}) = 0 \tag{8}$$

$$R_s R_w (1 + R_{c2})\frac{\partial t_s}{\partial z} - U_s(t_1 - t_s) = 0 \tag{9}$$

where the Péclet number $Pe = \dot{W}_1 L/DA_q$. Pe appears only in the differential equation for describing the shellside temperature. If $Pe \to \infty$, equation (6) approaches to the same as that [2] derived from the conventional plug-model on the condition that $R_s = 0$. The possibility that $Pe \to 0$ means that the longitudinal complete mixing occurs on the shell side. Generally, the shellside flow pattern lies between complete mixing and plug-flow, so that $0 < Pe < \infty$. Therefore, one can describe the effect of shellside flow maldistributions by means of Pe.

The uniform initial conditions take the following forms:

$$t_1(x,0) = t_s(x,0) = 0, \quad t_{2i}(x,0) = t_{wi}(x,0) = 0 \quad (i = 1,2,\ldots,N). \tag{10}$$

With regard to the dispersion model, the shellside inlet condition should appear as follows [8]:

$$t_1 - \frac{1}{Pe}\frac{\partial t_1}{\partial x} = f_1(z) \quad \text{at} \quad x = 0 \tag{11}$$

which is different from that [2] in the plug-flow model. The additional shellside exit condition must be supplemented. According to the second law of thermodynamics, its form will be [8]

$$\frac{\partial t_1}{\partial x} = 0 \quad \text{at} \quad x = 1. \tag{12}$$

The other N boundary and interface conditions corresponding to the tubeside temperature profiles are listed in Table 1. They vary with the number of tubeside passes and flow arrangements.

Functions $f_1(z)$ and $f_2(z)$ describe any possible inlet temperature changes on both sides of the exchanger, which may take place separately or simultaneously.

THEORETICAL SOLUTION

Owing to its simplicity, the Laplace transform is used in determining the solution to the system consisting of $(2N+2)$ differential equations. Using s as the Laplace parameter with respect to the dimensionless time variable z, one can easily obtain the following transformed equations:

$$\frac{1}{Pe}\frac{d^2T_1}{dx^2} - \frac{dT_1}{dx} = \left(s + U_1 - \sum_{i=1}^{N}\frac{U_1\varepsilon_{1i}\alpha_{1i}}{\alpha_{1i}+\alpha_{2i}+R_{wi}s} + U_s - \frac{U_s^2}{R_sR_w(1+R_{c2})+U_s}\right)T_1 - \sum_{i=1}^{N}\frac{U_1\varepsilon_{1i}\alpha_{2i}}{\alpha_{1i}+\alpha_{2i}+R_{wi}s}T_{2i} \tag{13}$$

$$\frac{dT_{2i}}{dx} = \operatorname{sign}\frac{U_2\varepsilon_{2i}\alpha_{1i}}{\alpha_{1i}+\alpha_{2i}+R_{wi}s}T_1 + \operatorname{sign}\left(\frac{U_2\varepsilon_{2i}\alpha_{2i}}{\alpha_{1i}+\alpha_{2i}+R_{wi}s} - \varepsilon_{ci}R_ts - U_2\varepsilon_{2i}\right)T_{2i} \quad (i = 1,2,\ldots,N) \tag{14}$$

$$T_{wi} = \frac{\alpha_{1i}T_1 + \alpha_{2i}T_{2i}}{\alpha_{1i}+\alpha_{2i}+R_{wi}s} \quad (i = 1,2,\ldots,N) \tag{15}$$

$$T_s = \frac{U_sT_1}{R_sR_w(1+R_{c2})s+U_s}. \tag{16}$$

Equations (13) and (14) can be transformed into a system of first-order equations. This is accomplished by introducing

$$\tilde{T}_1 = \frac{dT_1}{dx}. \tag{17}$$

In matrix notation this system appears in the form

$$\frac{d\mathbf{T}}{dx} = \mathbf{A}\mathbf{T} \tag{18}$$

where $\mathbf{T} = (T_{21}, T_{22}, \ldots, T_{2N}, T_1, \tilde{T}_1)^T$ and $\mathbf{A}$ is a matrix of $(N+2)$ order, the elements of which are given as

$$a_{ij} = \begin{cases} \operatorname{sign}\left(\dfrac{U_2\varepsilon_{2i}\alpha_{2i}}{\alpha_{1i}+\alpha_{2i}+R_{wi}s} - \varepsilon_{ci}R_ts - U_2\varepsilon_{2i}\right) & j = i \\ \operatorname{sign}\dfrac{U_2\varepsilon_{2i}\alpha_{1i}}{\alpha_{1i}+\alpha_{2i}+R_{wi}s} & j = N+1 \quad i \leqslant N, j \leqslant N+2 \\ 0 & \text{other } j \end{cases}$$

$$a_{N+1,j} = \begin{cases} 1 & j = N+2 \\ 0 & \text{other } j \end{cases} \qquad j \leqslant N+2$$

$$a_{N+2,j} = \begin{cases} -\dfrac{PeU_1\varepsilon_{1j}\alpha_{2j}}{\alpha_{1j}+\alpha_{2j}+R_{wj}s} & j \leqslant N \\ Pe\left(s + U_1 - \displaystyle\sum_{i=1}^{N}\frac{U_1\varepsilon_{1i}\alpha_{1i}}{\alpha_{1i}+\alpha_{2i}+R_{wi}s} + U_s - \frac{U_s^2}{R_sR_w(1+R_{c2})s+U_s}\right) & (j = N+1) \\ Pe & j = N+2 \end{cases}$$

According to the similar procedure described in ref. [8], a general solution to the system (18) is derived as

$$T = \sum_{j=1}^{N+2} d_jB_j\exp(\lambda_jx) \tag{19}$$

where λ_j $(j = 1,2,\ldots,N+2)$ are eigenvalues of matrix

Table 1. The boundary and interface conditions for $t_{2i}(x,z)$

			Tubeside flow arrangement	
	$x = 0,\ z \geqslant 0$	$x = 1,\ z \geqslant 0$	I	II
N even	$t_{2i} = t_{2i+1} = t_{2i,i+1}$ $i = 2,4,\ldots,N-2$	$t_{2i} = t_{2i+1} = t_{2i,i+1}$ $i = 1,3,\ldots,N-1$	$t_{2N}(0,z) = f_2(z)$	$t_{21}(0,z) = f_2(z)$
N odd	$t_{2i} = t_{2i+1} = t_{2i,i+1}$ $i = 2,4,\ldots,N-1$	$t_{2i} = t_{2i+1} = t_{2i,i+1}$ $i = 1,3,\ldots,N-2$	$t_{2N}(1,z) = f_2(z)$	$t_{21}(0,z) = f_2(z)$

A and $B_j = (b_{1j}, b_{2j}, \ldots, b_{N+2,j})^T$ are the corresponding eigenvalues. It should be emphasized that the solution (19) may fail, if multiple eigenvalues occur. In such cases that not all eigenvalues are distinct, a form of the solution is suggested in ref. [8]. d_j are $(N+2)$ unknown coefficients which must be determined subject to the given boundary conditions. From equation (19) and the given boundary conditions, one can readily build a matrix equation which confines these coefficients

$$\mathbf{WD} = \mathbf{G} \tag{20}$$

where $\mathbf{D} = (d_1, d_2, \ldots, d_{N+2})^T$ and $\mathbf{G} = (0, 0, \ldots, F_2(s), F_1(s))^T$, if the inlet boundary conditions on both sides are laid in the proper positions of the last two equations in equation (20). $\mathbf{W}$ is a $(N+2) \times (N+2)$ matrix whose elements depend on many factors such as the number of tubeside passes, the tubeside flow arrangement, the multiplicity of eigenvalues λ_j and the forms of shellside inlet and exit boundary conditions. Therefore, the coefficient vector $\mathbf{D}$ is determined as

$$\mathbf{D} = \mathbf{W}^{-1}\mathbf{G}. \tag{21}$$

So far the temperature profiles in the Laplace image-domain have been found. The shellside and tubeside temperature distributions can be explicitly expressed, respectively

$$T_1(x,s) = \sum_{j=1}^{N+2} d_j b_{N+1,j} \exp(\lambda_j x) \tag{22}$$

$$T_{2i}(x,s) = \sum_{j=1}^{N+2} d_j b_{ij} \exp(\lambda_j x) \quad (i = 1, 2, \ldots, N). \tag{23}$$

The temperature profiles T_{wi} and T_s have been already given by equations (15) and (16). Especially, the shellside exit response T_{1e} is determined from equation (22)

$$T_{1e} = \sum_{j=1}^{N+2} d_j b_{N+1,j} \exp(\lambda_j) \tag{24}$$

and the tubeside exit response T_{2e} varies with the tubeside flow arrangement. For tubeside flow arrangement I

$$T_{2e} = T_{21} = \sum_{j=1}^{N+2} d_j b_{1j}. \tag{25}$$

Otherwise, for tubeside flow arrangement II

$$T_{2e} = T_{2N} = \begin{cases} \sum_{j=1}^{N+2} d_j b_{Nj} & \text{even } N \\ \sum_{j=1}^{N+2} d_j b_{Nj} \exp(\lambda_j) & \text{odd } N \end{cases}. \tag{26}$$

In all these equations, d_j, B_j and λ_j may be functions of the Laplace parameter s. The inverse transform must be performed to obtain the final solution in the real time-domain. Obviously, it is impossible to finish this task analytically. A method of a numerical inverse Laplace transform called the Gaver–Stehfest [9] is appropriate for determining the transient responses to arbitrary inlet temperature changes in the time-domain. This numerical algorithm can be described by the following expressions

$$f(z) = \frac{\ln 2}{z} \sum_{i=1}^{M} K_i F\left(\frac{\ln 2}{z} i\right)$$

$$K_i = (-1)^{i+M/2} \times \sum_{k=(i+1)/2}^{\min(i, M/2)} \frac{K^{M/2}(2K)!}{(M/2-K)!K!(K-1)!(i-K)!(2K-i)!} \tag{27}$$

where M is the number of series terms to be summed and it must be even. The word 'min' means that the number of summed terms takes the lower of i and $M/2$. By means of expression (27), one can obtain the transient temperature profiles of both fluids, the core wall and the shell wall

$$t_j(x,z) = \frac{\ln 2}{z} \sum_{i=1}^{\min(i, M/2)} K_i T_j\left(x, \frac{\ln 2}{z} i\right) \tag{28}$$

where the subscript j can take 1, 2i, wi and s.

APPLICATIONS AND DISCUSSIONS

In order to expound the utility of the method developed in this paper and the influence of the thermal capacity of the shell as well as the difference between the dispersion and the plug-flow model, a number of examples are calculated for the condition where $U_1 = U_2$ and $R_r = 1.0$. These examples of the exit transient responses to arbitrary inlet temperature changes are examined for the shell and tube heat exchangers with different tubeside passes and flow arrangements, different distributions of $(hA)_1$ as well as $(hA)_2$ among tubeside passes and different ratios of the thermal capacity of the shell wall to that of the core wall.

Figure 2 shows the exit temperature responses to a shellside step inlet temperature change in a 1–2 heat exchanger with tubeside flow arrangement I. Figure 3 illustrates the superposition of exit responses to a tubeside step and a shellside exponential inlet change in a 1–6 heat exchanger with flow arrangement II. As a measure to check whether the afore-derived formulae are correct, the overall energy balance between both fluids has been examined. The results have shown that a precise energy balance under the steady state for the step inlet temperature change exists. Further, the calculation has been also performed for the case where $Pe \to \infty$ and the same results are obtained as those from the plug-flow model [2].

To investigate the influence of the thermal capacity of the shell wall and the effect of shellside maldistributions, the following definitions are introduced:

$$\delta_{1,2s} = \left|\frac{t_{1,2s} - t_{1,2}}{t_{1,2s}}\right| \quad \text{and} \quad \delta_{1,2P} = \left|\frac{t_{1,2P} - t^*_{1,2}}{t_{1,2P}}\right| \tag{29}$$

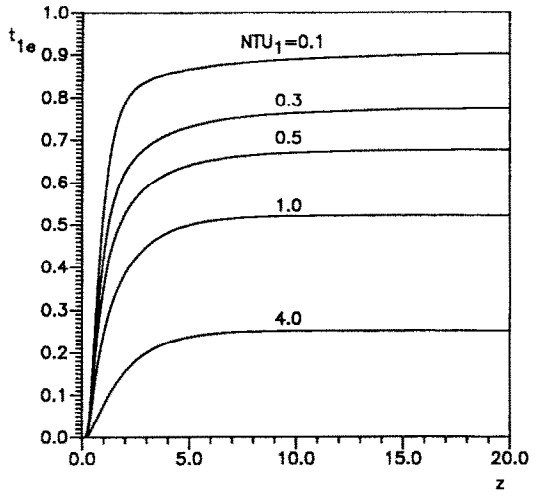

(a) shellside fluid

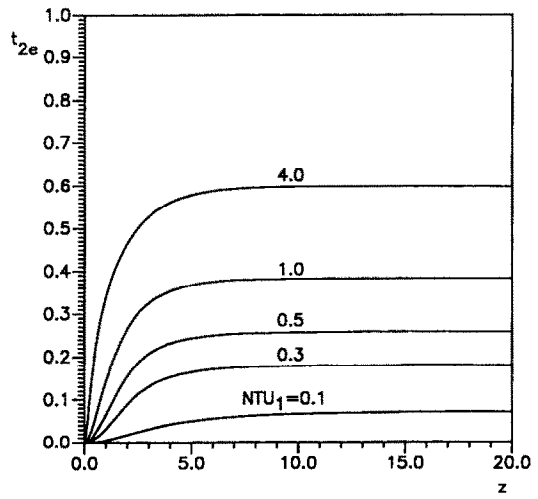

(b) tubeside fluid

FIG. 2. Exit responses to a shellside step inlet temperature change of a heat exchanger with counterflow arrangement ($R_1 = 0.8$, $R_w = R_s = 0.5$, coef = 0.2, $Pe = 4.0$, $f_1(z) = 1$, $f_2(z) = 0$). (a) Shellside fluid and (b) tubeside fluid.

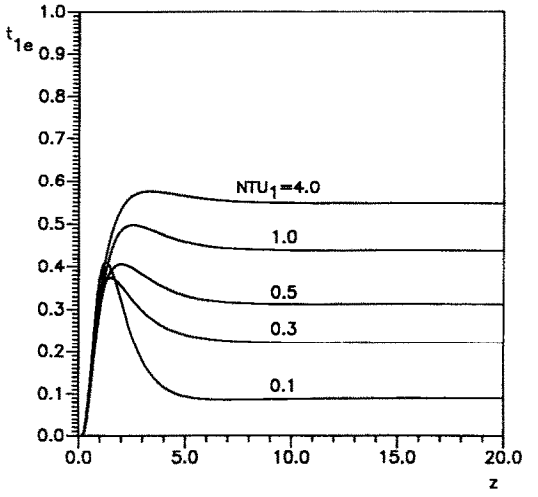

(a) shellside fluid

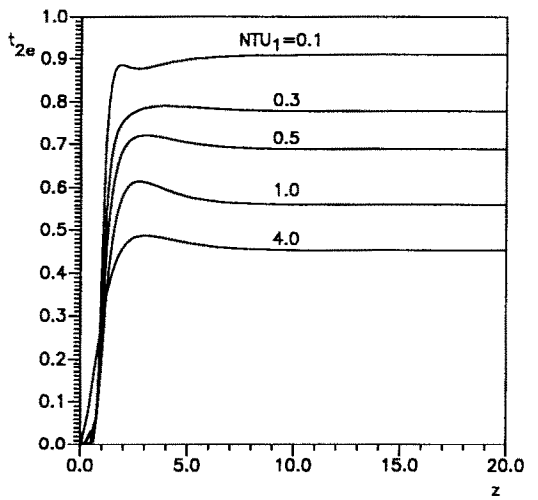

(b) tubeside fluid

FIG. 3. Superposition of exit responses to a shellside exponential and a tubeside step inlet temperature change of a 1–6 heat exchanger with tubeside flow arrangement II ($\varepsilon_{11} = \varepsilon_{14} = 0.2$, $\varepsilon_{12} = \varepsilon_{13} = \varepsilon_{15} = \varepsilon_{16} = 0.15$, $\varepsilon_{21} = \varepsilon_{24} = 0.2$, $\varepsilon_{22} = \varepsilon_{23} = \varepsilon_{25} = \varepsilon_{26} = 0.15$, $\varepsilon_{c1} = \varepsilon_{c4} = 0.2$, $\varepsilon_{c2} = \varepsilon_{c3} = \varepsilon_{c5} = \varepsilon_{c6} = 0.15$, $\varepsilon_{w1} = \varepsilon_{w4} = 0.2$, $\varepsilon_{w2} = \varepsilon_{w3} = \varepsilon_{w5} = \varepsilon_{w6} = 0.15$, $R_1 = 1.0$, $R_w = 0.5$, $R_s = 0.3$, coef = 0.1, $Pe = 6.0$, $f_1(z) = \exp(-t)$, $f_2(z) = 1$). (a) Shellside fluid and (b) tubeside fluid.

where $t_{1,2}$ and $t_{1,2P}$ are the dimensionless shellside and tubeside exit temperature responses without considering the shell wall, $t^*_{1,2}$ is the corresponding results from the plug-flow model [2] and $t_{1,2s}$ the ones calculated from the algorithm developed in this paper. Figures 4 and 5 illustrate the influence of the thermal capacity of the shell wall on the transient behaviour of heat exchangers, which depends upon the values of the thermal capacity and the heat transfer coefficient between the shell wall and shellside fluid as well as the lapse of time in the transient process. The results show that the thermal capacity of the shell wall should not be neglected, if the ratio $R_s = C_s/C_w > 0.1$ and coef $= U_s/U_1 > 0.1$. This effect passes approximately into nothingness, if the dimensionless time $z > 15$.

The examples plotted in Figs. 6 and 7 explain the effect of the shellside flow maldistributions. Because of such maldistributions, the exit responses occur earlier compared with the results from the plug-flow model. The smaller the Pe, the greater the time of lead, which means that the shellside flow maldistributions accelerate the shellside exit response. In fact, the smaller value of Pe corresponds to the stronger longitudinal mixing on the shell side. In such a case, the maldistributions will result in a greater shellside and a

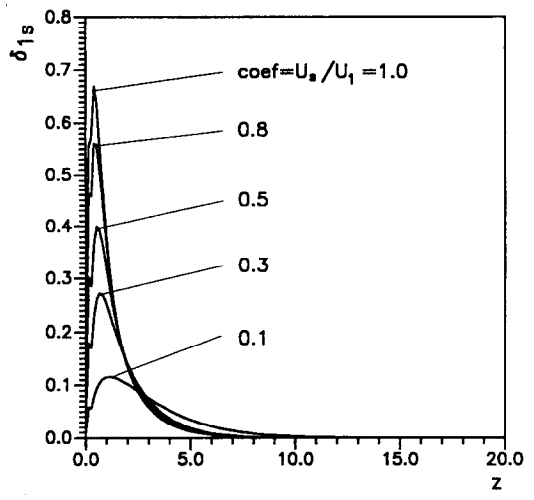

(a) shellside fluid

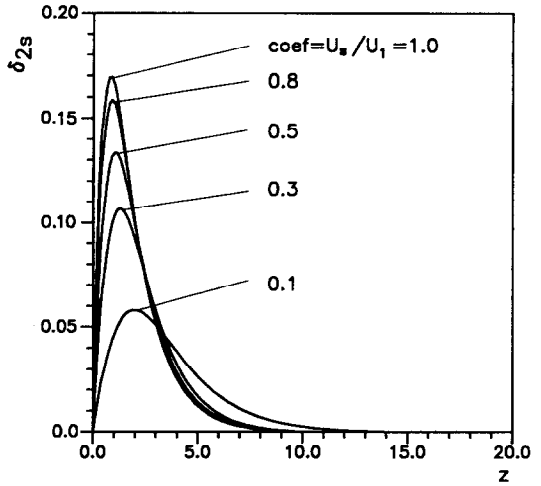

(b) tubeside fluid

FIG. 4. Influence of the parameter U_s on the exit responses to a shellside step inlet temperature change of a 1–4 heat exchanger with tubeside flow arrangement I ($\varepsilon_{11} = \varepsilon_{12} = \varepsilon_{13} = \varepsilon_{14} = 0.25$, $\varepsilon_{21} = \varepsilon_{22} = \varepsilon_{23} = \varepsilon_{24} = 0.25$, $\varepsilon_{c1} = \varepsilon_{c2} = \varepsilon_{c3} = \varepsilon_{c4} = 0.25$, $\varepsilon_{w1} = \varepsilon_{w2} = \varepsilon_{w3} = \varepsilon_{w4} = 0.25$, $R_1 = 0.8$, $R_w = 0.6$, $R_s = 0.4$, $NTU_1 = 1.5$, $Pe = 4.0$, $f_1(z) = 1$, $f_2(z) = 0$). (a) Shellside fluid and (b) tubeside fluid.

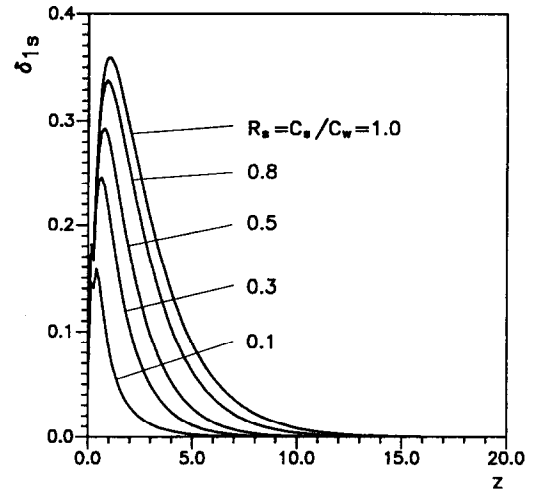

(a) shellside fluid

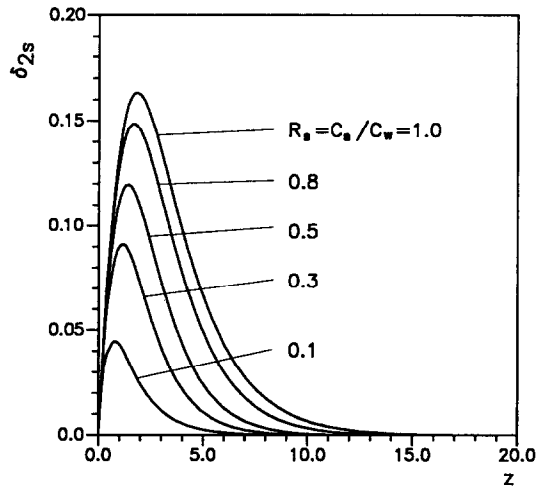

(b) tubeside fluid

FIG. 5. Influence of the thermal capacity of the shell wall on the exit responses to a shellside step inlet temperature change of a 1 4 heat exchanger with tubeside flow arrangement I ($\varepsilon_{11} = \varepsilon_{12} = \varepsilon_{13} = \varepsilon_{14} = 0.25$, $\varepsilon_{21} = \varepsilon_{22} = \varepsilon_{23} = \varepsilon_{24} = 0.25$, $\varepsilon_{c1} = \varepsilon_{c2} = \varepsilon_{c3} = \varepsilon_{c4} = 0.25$, $\varepsilon_{w1} = \varepsilon_{w2} = \varepsilon_{w3} = \varepsilon_{w4} = 0.25$, $R_1 = 0.8$, $R_w = 0.6$, $NTU_1 = 1.5$, coef = 0.3, $Pe = 4.0$, $f_1(z) = 1$, $f_2(z) = 0$). (a) Shellside fluid and (b) tubeside fluid.

smaller tubeside response. In other words, the maldistributions degrade the heat transfer process and a smaller temperature change through the apparatus follows. After the threshold of time, the effect of the maldistribution does not vary with time. This threshold value depends mainly on such parameters as Pe and NTU.

Furthermore, it should be underlined that because of the limitation of the Gaver–Stehfest algorithm, the above method can be used for predicting the transient responses to such arbitrary inlet temperature changes that have no discontinuities or rapid oscillations. One should be careful of its application to the transient response subject to the inlet temperature change which has oscillatory components.

NON-UNIFORM INITIAL CONDITIONS

The above-mentioned algorithm is based on the uniform initial conditions (10). It will be of more practical applications if the preceding method can be extended to the cases of non-uniform initial conditions. In general, a new transient process may follow the steady state whose temperature profiles such as $g_1(x)$, $g_{2i}(x)$, $g_{wi}(x)$ and $g_s(x)$ are the solutions to equations (6)–(9) as $\tau \to \infty$. Therefore, the initial

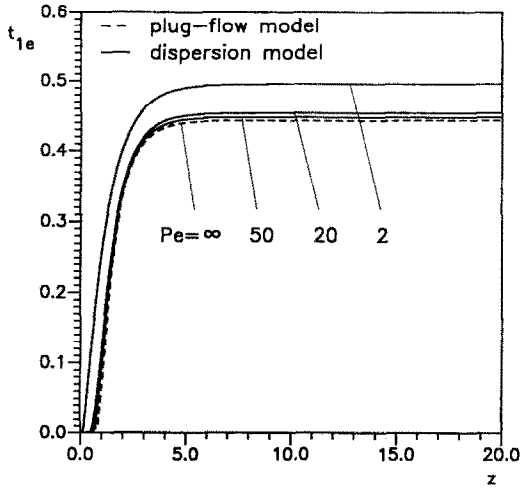

(a) shellside fluid

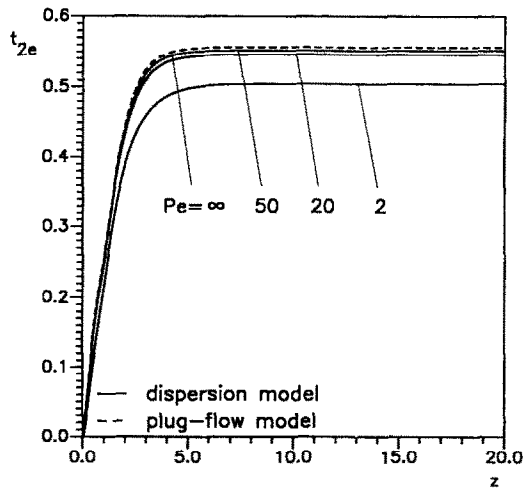

(b) tubeside fluid

FIG. 6. Comparison between the dispersion and plug-flow model in a 1–2 heat exchanger with tubeside flow arrangement I ($\varepsilon_{11} = \varepsilon_{12} = 0.5$, $\varepsilon_{21} = \varepsilon_{22} = 0.5$, $\varepsilon_{c1} = \varepsilon_{c2} = 0.5$, $\varepsilon_{w1} = \varepsilon_{w2} = 0.5$, $R_1 = 1.0$, $R_w = 0.5$, $NTU_1 = 2.0$, $R_s = 0$, coef = 0, $f_1(z) = 1$, $f_2(z) = 0$). (a) Shellside fluid and (b) tubeside fluid.

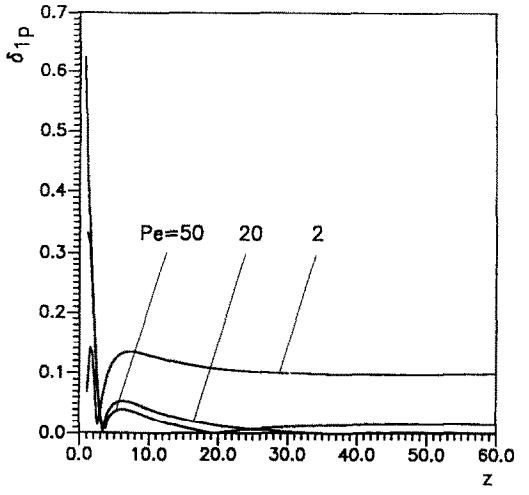

(a) shellside fluid

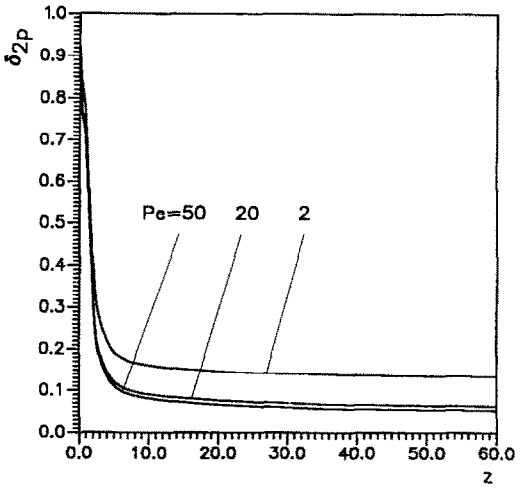

(b) tubeside fluid

FIG. 7. Difference between the calculated exit responses from the dispersion and plug-flow model in a 1–2 heat exchanger with tubeside flow arrangement I (the same parameters as those in Fig. 6).

conditions pertinent to the new transient process are described as follows:

$$t_1(x,0) = g_1(x), \quad t_s(x,0) = g_s(x),$$
$$t_{2i}(x,0) = g_{2i}(x), \quad t_{wi}(x,0) = g_{wi}(x)$$
$$(i = 1, 2, \ldots, N). \tag{30}$$

Then, the temperature profiles of the new transient process can be given as follows:

$$t_j(x,z) = g_j(x) + \phi_j(x,z) \tag{31}$$

where the subscript j can take 1, $2i$, wi and s. As already pointed out, $g_j(x)$ are the known steady solutions to the previous transient process as $\tau \to \infty$ and one only needs to determine the transient parts $\phi_j(x,z)$ in equation (31). The substitution of the transformation (31) into equations (6)–(9) reveals that $\phi_j(x,z)$ are the solutions of the following differential equations:

$$\frac{1}{Pe}\frac{\partial^2\phi_1}{\partial x^2} - \frac{\partial\phi_1}{\partial x} - \frac{\partial\phi_1}{\partial z} - \sum_{i=1}^{N} U_{1i}(\phi_1 - \phi_{wi}) - U_s(\phi_1 - \phi_s) = 0 \tag{32}$$

$$\text{sign}\frac{\partial\phi_{2i}}{\partial x} + \varepsilon_{ci}R_\tau\frac{\partial\phi_{2i}}{\partial z} + U_{2i}(\phi_{2i} - \phi_{wi}) = 0 \tag{33}$$

$$R_{wi}\frac{\partial\phi_{wi}}{\partial z} - \alpha_{1i}(\phi_1 - \phi_{wi}) - \alpha_{2i}(\phi_{2i} - \phi_{wi}) = 0 \tag{34}$$

Table 2. The boundary and interface conditions for $\phi_{2i}(x,z)$

			Tubeside flow arrangement	
	$x=0,\ z\geqslant 0$	$x=1,\ z\geqslant 0$	I	II
N even	$\phi_{2i}=\phi_{2i+1}=\phi_{2i,i+1}$ $i=2,4,\ldots,N-2$	$\phi_{2i}=\phi_{2i+1}=\phi_{2i,i+1}$ $i=1,3,\ldots,N-1$	$\phi_{2N}(0,z)=f_{2n}(z)-g_{2N}(0)$	$\phi_{21}(0,z)=f_{2n}(z)-g_{21}(0)$
N odd	$\phi_{2i}=\phi_{2i+1}=\phi_{2i,i+1}$ $i=2,4,\ldots,N-1$	$\phi_{2i}=\phi_{2i+1}=\phi_{2i,i+1}$ $i=1,3,\ldots,N-2$	$\phi_{2N}(1,z)=f_{2n}(z)-g_{2N}(1)$	$\phi_{21}(0,z)=f_{2n}(z)-g_{21}(0)$

$$R_s R_w(1+R_{c2})\frac{\partial\phi_s}{\partial z}-U_s(\phi_1-\phi_s)=0. \quad (35)$$

From equation (30) one can obtain the uniform initial conditions subject to equations (32)–(35) with the substitution of equation (31)

$$\phi_1(x,0)=\phi_s(x,0)=0,\quad \phi_{2i}(x,0)=\phi_{wi}(x,0)=0 \quad (i=1,2,\ldots,N). \quad (36)$$

Similarly, the boundary conditions for the shellside temperature are derived

$$\phi_1-\frac{1}{Pe}\frac{\partial\phi_1}{\partial x}=f_{1n}(z)-g_1+\frac{1}{Pe}\frac{\mathrm{d}g_1}{\mathrm{d}x} \quad \text{at} \quad x=0$$

$$\text{and} \quad \frac{\partial\phi_1}{\partial x}=-\frac{\mathrm{d}g_1}{\mathrm{d}x}=0 \quad \text{at} \quad x=1. \quad (37)$$

The boundary and interface conditions for $\phi_{2i}(x,z)$ are listed in Table 2.

Obviously, this system of differential equations is similar to the one consisting of equations (6)–(9) as well as the shellside boundary conditions (11), (12) and the tubeside conditions listed in Table 1. Therefore, the afore-derived algorithm can be directly used to find the transient parts $\phi_j(x,z)$ according to equations (32)–(35) subject to the corresponding initial and boundary conditions without difficulty. The final temperature responses $t_j(x,z)$ to the new inlet temperature changes $f_{1n}(z)$ and $f_{2n}(z)$ under the non-uniform initial conditions can be easily obtained by means of the superposition (equation (31)).

CONCLUSIONS

On the basis of the dispersion model instead of the conventional plug-flow model, a method has been developed to predict the transient behaviour of multipass shell and tube heat exchangers, considering the shellside flow maldistributions. In addition to the thermal capacities of both fluids and the core wall, the thermal capacity of the shell wall has been included to derive the more universal formulae which are applicable to the analysis of the transient behaviour subject to arbitrary inlet temperature changes. Such changes may take place on either side or simultaneously on both sides.

The influence of the thermal capacity of the shell wall should not be neglected as usual, if the values of R_s and coef lie in the ranges $R_s > 0.1$ and coef > 0.1. The shellside flow maldistributions result in a quicker exit temperature response which cannot be explained with the plug-flow model. The Péclet number Pe quantitatively describes the effect of the shellside flow maldistributions. The influence of the maldistributions on the transient behaviour does not vary with time, if the dimensionless time z exceeds a threshold value which depends upon such parameters as Pe and NTU, etc. In the case that $Pe\to\infty$, the dispersion model approaches to the plug-flow model. By means of the principle of superposition, the method developed in this paper can be readily extended to cases of the non-uniform initial conditions.

Acknowledgement—The authors would like to express their thanks to the 'Deutsche Forschungsgemeinschaft' for the financial support of this research project.

REFERENCES

1. D. J. Correa and J. L. Marchetti, Dynamic simulation of shell-and-tube heat exchangers, *Heat Transfer Engng* **8**, 50–59 (1987).
2. W. Roetzel and Y. Xuan, Transient behaviour of multipass shell-and-tube heat exchangers, *Int. J. Heat Mass Transfer* **35**, 703–710 (1992).
3. A. C. Mueller, Effects of some types of maldistribution on the performance of heat exchangers, *Heat Transfer Engng* **8**, 75–86 (1987).
4. W. Roetzel and Y. Xuan, Dispersion model for divided-flow heat exchanger, design and operation of heat exchangers. In *Proc. Eurotherm Sem. No. 18*, Hamburg, 27 Feb.–1 March 1991, p. 103. Springer, Berlin (1991).
5. W. Roetzel and Y. Xuan, Dispersion model for split-flow heat exchanger. In *Recent Advances in Heat Transfer* (Edited by B. Sundén and A. Žukauskas), pp. 561–575. Elsevier, Amsterdam (1992).
6. S. G. Taylor, The dispersion of matter in turbulent flow through a pipe, *Proc. R. Soc.* **A223**, 447–468 (1954).
7. W. Roetzel and Y. Xuan, The effect of core longitudinal heat conduction on the transient behaviour of multipass shell and tube heat exchangers, *Heat Transfer Engng* (submitted).
8. Y. Xuan, *Thermische Modellierung mehrgängiger Rohrbündelwärmeübertrager mit Umlenkblechen und geteiltem Mantelstrom*, Fortschr.-Ber. VDI Reihe 19 Nr. 52. VDI, Düsseldorf (1991).
9. H. Stehfest, Numerical inversion of Laplace transforms, *Commun. ACM* **13**, 47–49 (1970).

ANALYSE DU COMPORTEMENT VARIABLE D'UN ECHANGEUR THERMIQUE MULTIPASSES TUBES-CALANDRE AVEC LE MODELE DE DISPERSION

Résumé—Afin de prendre en compte l'effet des mauvaises répartitions du fluide côté-calandre, on utilise le modèle de dispersion pour prédire le comportement variable soumis à des changements arbitraires de température d'entrée dans les échangeurs tubes-calandre. Le nombre et la taille des passes côté-tube sont arbitraires et deux arrangements possibles d'écoulement sont considérés. En plus des capacités thermiques des fluides et de la paroi intermédiaire, on inclut la capacité thermique de la calandre. La solution finale est obtenue à l'aide de la transformée numérique inverse de Laplace. On discute l'influence de la mauvaise distribution de l'écoulement côté-calandre et de la capacité thermique de la calandre.

UNTERSUCHUNG DES INSTATIONÄREN VERHALTENS VON MEHRGÄNGIGEN ROHRBÜNDELWÄRMEÜBERTRAGERN MIT DEM DISPERSIONSMODELL

Zusammenfassung—Um den Einfluß der Fehlverteilung der Strömung im Außenraum zu berücksichtigen, wird zur Vorausberechnung des instationären Verhaltens bei beliebigen Änderungen der Eintrittstemperaturen das Dispersionsmodell angewendet. Die Anzahl und Größe der Rohrdurchgänge ist beliebig, und es werden beide möglichen Schaltungsarten betrachtet. Neben den Wärmekapazitäten beider Fluide und der Trennwand wird auch die Kapazität des Mantels im Modell mit berücksichtigt. Die endgültige Lösung erhält man durch eine numerische Laplace-Rücktransformation. Es wird der Einfluß der Fehlverteilung im Außenraum und der Wärmekapazität des Mantels diskutiert.

АНАЛИЗ ПЕРЕХОДНЫХ ХАРАКТЕРИСТИК МНОГОХОДОВЫХ КОЖУХО-ТРУБНЫХ ТЕПЛООБМЕННИКОВ С ИСПОЛЬЗОВАНИЕМ ДИСПЕРСНОЙ МОДЕЛИ

Аннотация—Для учета структуры течения в кожухе используется дисперсная модель, по которой определяются переходные характеристики при произвольных изменениях температуры на входе в многоходовых кожухо–трубных теплообменниках. Количество и размеры переходов в трубах являются произвольными, при этом рассматриваются две возможные структуры течения. Наряду с теплоемкостями рабочих жидкостей и стенки центральной трубы в модели учитывается теплоемкость стенки кожуха. Решение получено методом численного обратного преобразования Лапласа. Исследуется влияние структуры течения в кожухе и теплоемкости стенки кожуха.